



Sensitivity Analysis of a Nonlinear Lumped Parameter Model of HIV Infection Dynamics

D. M. BORTZ AND P. W. NELSON*

Department of Mathematics,
University of Michigan,
2074 East Hall,
525 East University Avenue,
Ann Arbor, MI 48109-1109,
USA

E-mails: dmbortz@umich.edu; pwn@umich.edu

A formal sensitivity analysis is performed on a delay differential equation model for the viral dynamics of an *in vivo* HIV infection during protease inhibitor therapy. We present results of both a differential analysis as well as a principle component based analysis and provide evidence that suggests the exact times at which specific parameters have the most influence over the solution. We offer insight into the pairwise mathematical relationships between the productively infected T-cell death rate δ , the viral plasma clearance rate c , and the time delay τ between infection and viral production as they relate to the viral dynamics. The results support the claim that the presence of a nonzero delay has a major impact on the model dynamics. Lastly, we comment upon the inadequacies of an alternative principle component based analysis.

© 2003 *Society for Mathematical Biology*. Published by Elsevier Ltd. All rights reserved.

1. INTRODUCTION

For any dynamical system designed to model physical or biological phenomena, it is desirable to be able to characterize the nature of the connection between the system's parameters and the observed solution. These parameters are contrived to reflect specific aspects of the phenomena being studied (e.g., death rates for HIV infected CD4 T-cells), and thus it is advantageous to ascertain as much as possible about how perturbations in the parameters manifest themselves in the solution. Within the field of HIV modeling there are many papers that comment on this topic (Stilianakis *et al.*, 1997; Perelson and Nelson, 1999; Stafford *et al.*, 2000) by presenting the results of varying a chosen parameter and running the corresponding simulation. In this paper, we perform [on a recently published model by

*Author to whom correspondence should be addressed.

Nelson *et al.* (2001)] a formal *sensitivity analysis*, which is a mathematical approach designed to reveal information about the (possibly hidden and/or nonlinear) relationships between parameters and solutions. To our knowledge, this paper is the first work to apply these analytical sensitivity analysis techniques to HIV models as well as to discuss the mathematical connections between the parameters and their impact upon the viral dynamics.

This type of analysis was initially developed in the context of modern control theory and is commonly used in aerospace, chemical, electrical, and civil engineering. Moreover, a precursor to the idea can be traced back to an 1833 publication (Philosophical Transactions of the Royal Society) concerning the results of an electrostatics experiment measuring the inductance of certain metals (Christie, 1833). More recent developments can be found both in the literature of control theory and that of iterative optimization methods, where the approximation of analytical gradients and Hessians is sometimes necessary. There are many sensitivity analysis techniques that are more mathematically sophisticated than simply observing the output generated by varying a chosen parameter, and we will be using both a basic differential analysis approach as well as one based on the principle component analysis (PCA). For illustrations of these as well as more mathematically advanced methods, we recommend the following articles and books: Adelman and Haftka (1986), Banks and Bortz (2002), Eslami (1994), Frank (1978), Iman and Helton (1988), Kleiber *et al.* (1997), Lazarides *et al.* (1998, 1994), Saltelli *et al.* (2000), Vajda and Turányi (1986), Vajda *et al.* (1985), Wierzbicki (1984) and Zhou *et al.* (1998). Furthermore, we direct the interested reader specifically to Saltelli *et al.* (2000), which presents an excellent overview and introduction to many of the current sensitivity analysis tools and techniques.

2. SENSITIVITY EQUATIONS

Our model [originally from Nelson *et al.* (2001)] consists of the following system of coupled delay differential equations

$$\begin{aligned}\dot{T}^*(t) &= -\delta T^*(t) + kT_0 V_I(t - \tau), \\ \dot{V}_I(t) &= (1 - n_p)N\delta T^*(t) - cV_I(t), \\ \dot{V}_{NI}(t) &= n_p N\delta T^*(t) - cV_{NI}(t),\end{aligned}\tag{1}$$

where t is the independent time variable, T^* represents the productively infected T-cells, V_I is the infectious virus, V_{NI} is the noninfectious virus, and the initial conditions and other system parameters are described in Table 1. In order to enforce a constant steady-state history for V_I , we have set $k = \frac{c}{NT_0}$, and it is substituted below, where appropriate. Let us denote T_q^* , $V_{I,q}$, and $V_{NI,q}$ as the sensitivity

Table 1. Parameters and initial conditions for (1). The specific values of τ , δ , and c are from Nelson *et al.* (2001), which were calculated using a nonlinear least squares parameter estimation approach to fitting the data in Perelson *et al.* (1996).

Name	Description	Value (patient 103)
T_0	Target T-cell concentration	408 cells mm^{-3}
T_0^*	Initial productively infected T-cell concentration	0.1626 cells mm^{-3}
V_{I0}	Initial infectious viral concentration	28500 virions ml^{-1}
V_{NI0}	Initial noninfectious viral concentration	0 virions ml^{-1}
τ	Delay between infection and production	0.91 days
δ	Infected T-cell death rate	1.57/day
c	Viral clearance rate	4.3/day
N	Burst size	480virions/cell
n_p	Protease inhibitor efficacy	0.7

functions of T^* , V_I , and V_{NI} with respect to an arbitrary parameter q , that is

$$T_q^*(t) = \frac{\partial}{\partial q} T^*(t, q),$$

$$V_{I,q}(t) = \frac{\partial}{\partial q} V_I(t, q),$$

$$V_{NI,q}(t) = \frac{\partial}{\partial q} V_{NI}(t, q),$$

for all t . Previous work has shown that the dynamics of viral infection after the start of anti-viral therapy are predominantly controlled by δ and c (Perelson *et al.*, 1996; Perelson and Nelson, 1999) and τ (Nelson *et al.*, 2000, 2001; Nelson and Perelson, 2002). The corresponding sensitivity systems with respect to δ , c , and τ are

$$\dot{T}_\delta^*(t, \delta) = -\delta T_\delta^*(t, \delta) + kT_0 V_{I,\delta}(t - \tau, \delta) - T^*(t, \delta),$$

$$\dot{V}_{I,\delta}(t, \delta) = (1 - n_p)N\delta T_\delta^*(t, \delta) - cV_{I,\delta}(t, \delta) + (1 - n_p)NT^*(t, \delta),$$

$$\dot{V}_{NI,\delta}(t, \delta) = n_p N\delta T_\delta^*(t, \delta) - cV_{NI,\delta}(t, \delta) + n_p NT^*(t, \delta),$$

and

$$\dot{T}_c^*(t, c) = -\delta T_c^*(t, c) + kT_0 V_{I,c}(t - \tau, c) + \frac{1}{N} V_I(t - \tau, c),$$

$$\dot{V}_{I,c}(t, c) = (1 - n_p)N\delta T_c^*(t, c) - cV_{I,c}(t, c) - V_I(t, c),$$

$$\dot{V}_{NI,c}(t, c) = n_p N\delta T_c^*(t, c) - cV_{NI,c}(t, c) - V_{NI}(t, c),$$

and

$$\dot{T}_\tau^*(t, \tau) = -\delta T_\tau^*(t, \tau) + kT_0 V_{I,\tau}(t - \tau, \tau) - kT_0 \dot{V}_I(t - \tau, \tau),$$

$$\dot{V}_{I,\tau}(t, \tau) = (1 - n_p)N\delta T_\tau^*(t, \tau) - cV_{I,\tau}(t, \tau),$$

$$\dot{V}_{NI,\tau}(t, \tau) = n_pN\delta T_\tau^*(t, \tau) - cV_{NI,\tau}(t, \tau),$$

respectively.

The ideas behind calculating the sensitivity equations originate from regular perturbation theory, and indeed, the sensitivity solutions are actually the coefficients of the first order truncation of the Taylor series for the original state functions [see Sections 6 and 7 in [Lin and Segel \(1988\)](#)]. These Taylor series (and thus the equations) are derived by treating a parameter as another independent variable and expanding the series around the best fit value for that parameter. In other words, the sensitivity solutions should be viewed as the Fréchet derivatives in the ‘direction’ of the chosen parameter [see [Banks and Bortz \(2002\)](#) or Section 3.3.2 of [Bortz \(2002\)](#)]. When evaluated at time t , the value of the sensitivity function indicates the rate of change in the state with respect to the change in the chosen parameter. If $V_{I,\tau}(2, 0.5) = 100$, for example, this means that the derivative of the infectious virion compartment V_I with respect to the time delay τ at time $t = 2$ days and delay $\tau = 0.5$ days, is 100 virions per ml-days.

The semi-relative sensitivity solutions (depicted in [Fig. 2](#)) are calculated by simply multiplying the unmodified sensitivity solutions by a chosen parameter, e.g., $\tau V_{I,\tau}(t, \tau)$, which provides information concerning the amount the state will change when that parameter is doubled (i.e., a perturbation on the order of τ). The logarithmic sensitivity solutions depicted in [Fig. 3](#) [and which get their name from the fact that $\frac{\partial \log(V_I)}{\partial \log(\tau)}(t) = \frac{\tau}{V_{I,\tau}(t, \tau)} V_{I,\tau}(t, \tau)$] are dimensionless and thus indicate what percentage change can be expected from a doubling of the parameter (i.e., a 100% change). In general, it is best to calculate both types of sensitivity solutions to obtain a more thorough understanding of the dynamics.

3. DIFFERENTIAL ANALYSIS

We now present a basic differential sensitivity analysis of the equations in (1). We chose the data from one patient with which to illustrate the sensitivity analysis, as the study of other patients generated similar interpretations and conclusions. Both the observations of viral RNA concentrations from patient 103 [from [Perelson *et al.* \(1996\)](#)] and the best fits for $\delta = 1.57$ per day, $c = 4.3$ per day, and $\tau = 0.91$ days are depicted in [Fig. 1](#). The other parameters (including initial conditions) for patient 103 are depicted in [Table 1](#), and, as mentioned in the previous section, we set $k = \frac{c}{NT_0} = 2.1957e - 8$ ml per virion-days to ensure a steady-state history for V_I . All simulations were performed in Matlab using the delay differential equation solver **dde23** ([Shampine and Thompson, 2001](#)) on a Pentium IV 1.8 GHz Linux workstation.

The plots in [Fig. 2](#) depict, for the three state variables and the observed compartment, the semi-relative sensitivity solutions with respect to each of the three

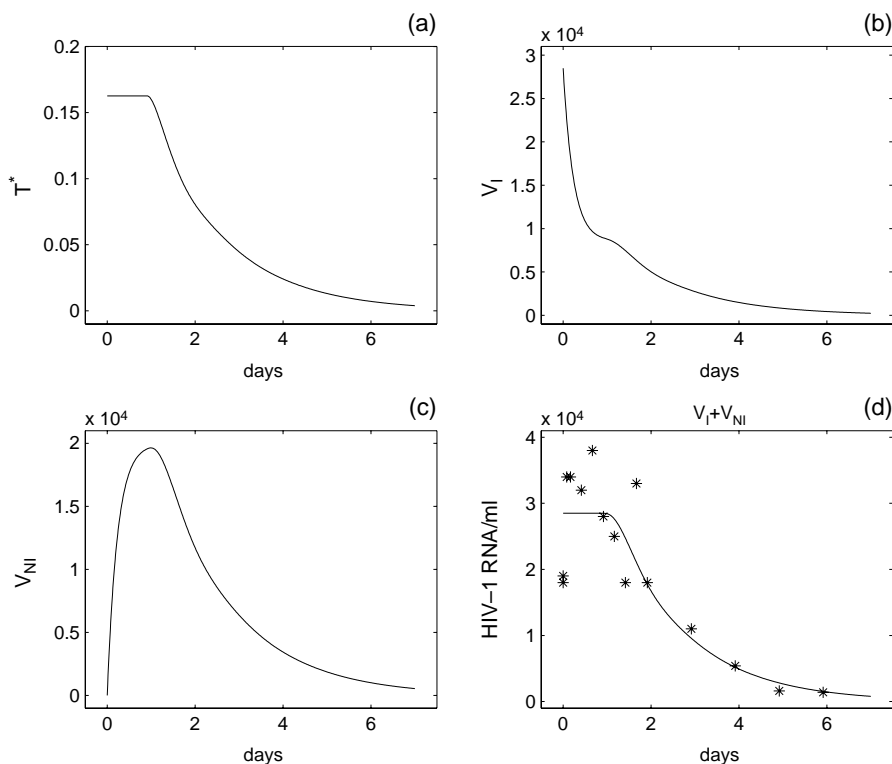


Figure 1. The simulation plots for the solution to (1) (best fit parameters from Table 1: $c = 4.3$ per day, $\delta = 1.57$ per day, and $\tau = 0.91$ days) of the infected T-cell concentration T^* , infectious viral concentration V_I , noninfectious viral concentration V_{NI} , and the comparison of total viral RNA concentration ($V_I + V_{NI}$) with the observed data from patient 103 are depicted in subfigures (a), (b), (c), and (d), respectively.

parameters of interest. It is important to realize that the information presented in these plots is not equivalent to simply calculating the difference between the solution in Fig. 1 and a solution to (1) with a slightly increased parameter, but instead the plots depict the derivative of the state with respect to the chosen parameter, as a function of time. We interpret the graph for $\delta T_\delta^*(t, \delta)$ in Fig. 2(a) to mean that the perturbation of δ exhibits its greatest influence over T^* early in the simulation, with an initial expected decrease in T^* of about 0.1 infected T-cells per mm^3 . Likewise, the graph of $c V_{I,c}(t, c)$ in Fig. 2(b) suggests that a doubling of c will yield a decrease of about 7300 infectious virus V_I (per ml) by time $t = 0.23$ days, but with a decreased effect over time. For the delay τ , a doubling will have no effect on any state until after one day, and, like the other parameters, the impact will gradually become negligible. It is clear, though, that a perturbation of the delay τ dramatically influences the solutions, with its greatest influence being felt just before time $t = 2$ days. This nontrivial impact on $V_I + V_{NI}$ between time $t = 1$ day and $t = 4$ days, moreover, strongly suggests that the presence of the delay could have an observable impact on the estimates of δ and/or c calculated in fitting the data

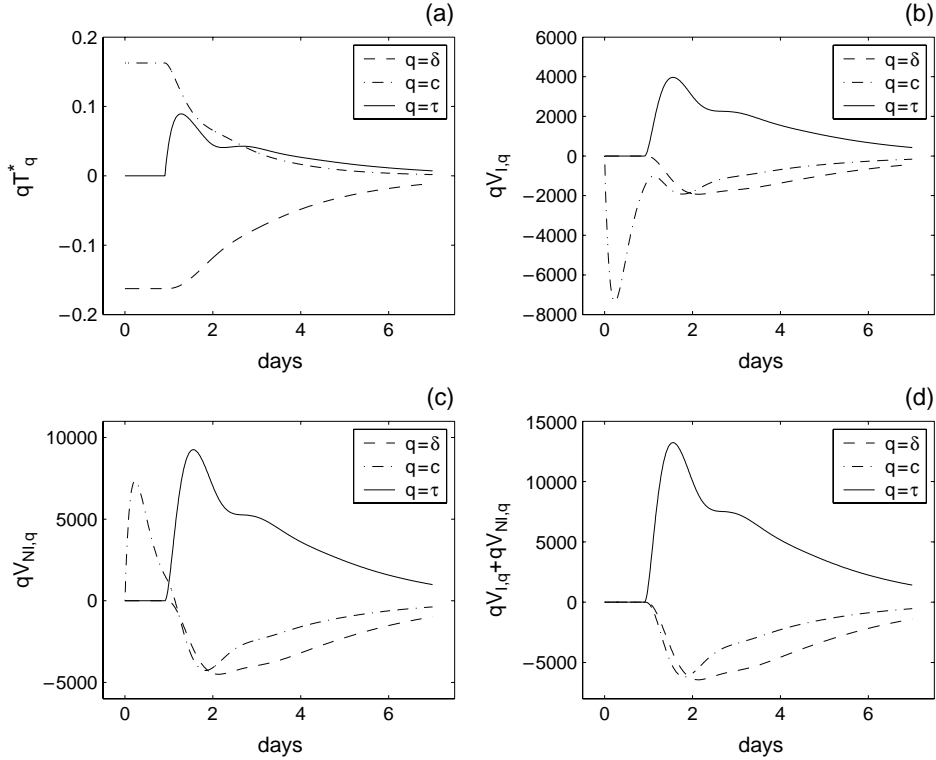


Figure 2. Semi-relative sensitivity solutions; note the initial impact of δ in δT_{δ}^* and c in $cV_{I,c}$, $cV_{NI,c}$, and $cV_{I,c} + cV_{NI,c}$ as well as the lack of influence of perturbations of τ until after day one.

(for further discussion, see Section 4). We note that perturbations of c strongly influence all compartments, as is depicted in Fig. 2(a), 2(b), and 2(c), respectively, however, the plot in Fig. 2(d) suggests that the initial impacts of c on V_I and V_{NI} cancel each other when compared with observed data.

The logarithmic sensitivity solutions with respect to each of the three parameters (δ , c , τ) for the three state variables and the observed compartment are depicted in Fig. 3. We interpret these plots to represent percentage changes in the solutions induced by positive perturbations of the parameters. These plots suggest that perturbations of δ have a negative impact upon the solutions, whereas perturbations of τ have a positive, yet delayed, impact. Moreover, at time $t = 7$ days, the plots suggest that perturbations of τ will cause a (roughly) 200% change in all solutions.

We note, however, that 200% changes, at time $t = 7$ days, in the solutions depicted in Fig. 1 are not significant due to the low level of concentration in all compartments at $t = 7$. As before, perturbations of c induce changes in V_I and V_{NI} , but the effects neutralize each other in the total viral concentration compartment.

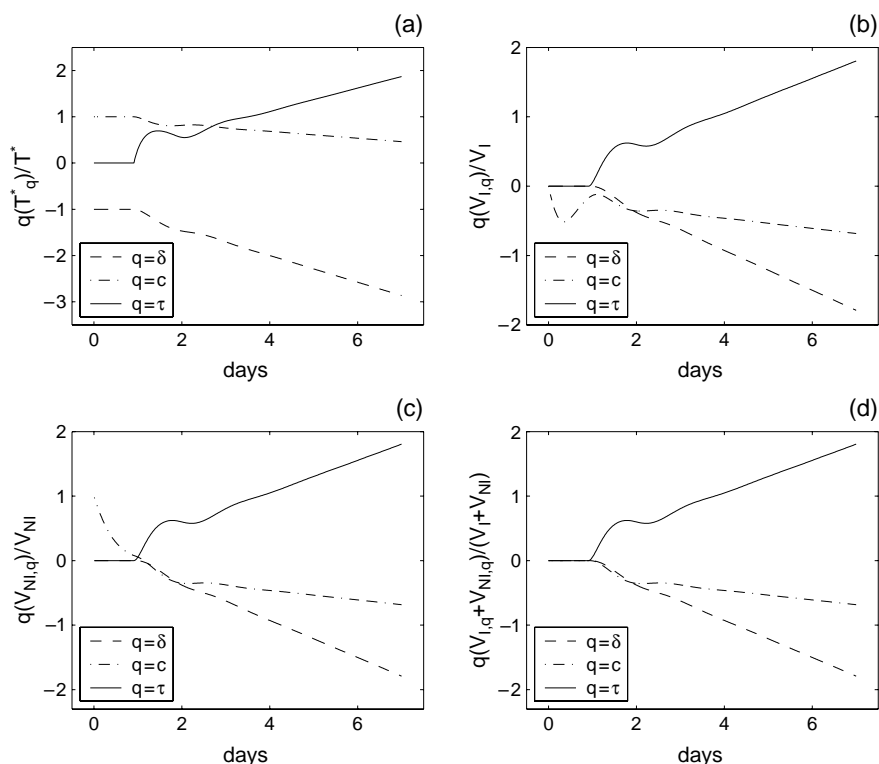


Figure 3. Logarithmic sensitivity solutions; note the negative impact of δ in all compartments, the initially neutralized impact of c in (d), and the delayed effect of τ in all compartments.

This basic differential sensitivity analysis has examined the effects of locally perturbing a handful of constitutive parameters of (1) near $\delta = 1.57$ per day, $c = 4.3$ per day, and $\tau = 0.91$ days. The analysis suggests that the infected T-cell death rate δ is the most influential over the infected T-cell population T^* and the viral clearance rate c has a large influence over the viral concentrations V_I and V_{NI} . Thus, the interpretation of this differential sensitivity analysis agrees with the commonly accepted understanding of the infection dynamics. We draw attention, however, to the fact that within the plots in Figs. 2 and 3, the delay τ impacts all compartments in a nontrivial manner. Again, this strongly suggests that the inclusion of a nonzero delay is crucial to the development of an accurate model, and that it might be prudent to view with some suspicion the accuracy of parameter estimates made using models without a delay.

4. PRINCIPAL COMPONENT ANALYSIS

The principal component analysis (PCA) based approach we present below is designed to reveal which parameter perturbations and/or combinations of

parameter perturbations induce the largest and smallest changes in the solution near the best fit parameters (in a least squares sense and for a given data set). Illustrations of the application of this sensitivity analysis technique to systems in other fields can be found in articles in the combustion and chemical physics journals referenced in the introduction.

4.1. Cost functional approximation. Let x be an m -dimensional vector valued function of time t and parameters $q \in \mathcal{Q}_{\text{ad}}$, where $\mathcal{Q}_{\text{ad}} \subset \mathbb{R}^n$ is the subspace of admissible parameters and q^* is the vector of best fit parameters. In order to measure the effects incurred by a variation of the parameters, we consider the relative least squares cost functional

$$J(q) = \int_{t_0}^{t_f} R(q; t)^T R(q; t) dt, \quad (2)$$

where

$$R(q; t) = [r_1(t, q, q^*) r_2(t, q, q^*) \cdots r_m(t, q, q^*)]^T$$

and

$$r_i(t, q, q^*) = \frac{x_i(t, q) - x_i(t, q^*)}{x_i(t, q^*)}. \quad (3)$$

Note that for our problem $x(t, q) = [T^*(t, q), V_I(t, q), V_{NI}(t, q)]^T$ and thus $m = 3$. We also remark that this cost functional is a weighted least squares functional with weights $1/x_i(t, q^*)^2$.

In general, J will be nonlinear in q , and thus we consider the Taylor series of J in order to study the local behavior around q^*

$$J(q) = J(q^*) + \nabla J(q^*)(\Delta q) + \frac{1}{2}(\Delta q)^T (\nabla^2 J(q^*))(\Delta q) + \cdots,$$

where $\Delta q = q - q^*$, and ∇J and $\nabla^2 J$ are the gradient of J and the Hessian of J , respectively. Note that since J measures the distance of a solution to the best fit solution, q^* is a minimizer of J , thus $J(q^*) = 0$ and $\nabla J(q^*) = 0$, and therefore a second order truncation of the series yields

$$J(q) \approx \frac{1}{2}(\Delta q)^T (\nabla^2 J(q^*))(\Delta q).$$

A well known fact from the theory of nonlinear least squares [see [Moré and Wright \(1993\)](#)] is that the computation of the Hessian of J evaluated at q^* is simply

$$\nabla^2 J(q^*) = 2 \int_{t_0}^{t_f} \left\{ R'(q^*; t)^T R'(q^*; t) + \sum_{i=1}^m r_i(t, q^*, q^*)^T (\nabla_q^2 r_i(t, q^*, q^*)) \right\} dt$$

where R' is the $m \times n$ Jacobian of R . The relative residual (3) evaluated at q^* is, however, zero and therefore it is not unreasonable to approximate $J(q)$, for q near q^* , by

$$J(q) \approx (\Delta q)^T \left\{ \int_{t_0}^{t_f} R'(q^*; t)^T R'(q^*; t) dt \right\} (\Delta q)$$

where the (i, j) th element of $R'(q^*; t)$ is $\left. \frac{1}{x_i(t, q)} \frac{\partial x_i(t, q)}{\partial q_j} \right|_{q=q^*}$ (the semi-relative sensitivity of the i th element of x with respect to the j th element of q and evaluated at q^*). It is this form of the approximation to J which we will use in our analysis below.

4.2. Eigenvalue decomposition. We know from results in Bellman and Cooke (1963) that there exists a unique solution to a system of equations of the form (1) and that it is continuous for $t \geq t_0$. Since the output we obtain from numerically solving (3) is only available at a discrete set of values of t , to crudely approximate the integral, we can choose a simple uniform partitioning of $[t_0, t_f]$ into p sub-intervals and add up a right side Riemann sum. If we let $\{t_j\}$ for $j = 0, 1, 2, \dots, p$ be the partition nodes of $[t_0, t_f]$ and $S_j(q) = R'(q; t_j)$, we find that

$$\begin{aligned} J(q) &\approx \frac{(t_f - t_0)}{p} \sum_{j=1}^p (\Delta q)^T S_j^T(q) S_j(q) (\Delta q) \\ &\approx \frac{(t_f - t_0)}{p} (\Delta q)^T \mathbf{S}_q^T \mathbf{S}_q (\Delta q) \end{aligned} \quad (4)$$

where

$$\mathbf{S}_q = \begin{bmatrix} S_1(q) \\ S_2(q) \\ \vdots \\ S_p(q) \end{bmatrix},$$

is commonly referred to as the *relative sensitivity matrix*. Since the cost functional (4) is clearly a quadratic function of Δq , we are interested in the ‘direction’ of Δq which locally incurs the greatest and smallest changes in J .

To illustrate our reasoning, we consider the generalized eigenvalue decomposition of $\mathbf{S}_q^T \mathbf{S}_q = U \Lambda U^T$, where $U = [u_1, u_2, \dots, u_n] \in \mathbb{R}^{n \times n}$ is orthonormal and the eigenvalues are on the diagonal of Λ . The substitution of the $U \Lambda U^T$ decomposition into (4) yields

$$J(q) \approx \frac{(t_f - t_0)}{p} (U^T \Delta q)^T \Lambda (U^T \Delta q),$$

which suggests that we should examine $U^T \Delta q$ closely. Similar to the development in Vajda *et al.* (1985), we define $\Psi = U^T q$, $\Delta \Psi = U^T (\Delta q)$, and denote Ψ as

a *principle component*. The i th element of $\Delta\Psi$ is the \mathbb{R}^n inner product $\langle u_i, \Delta q \rangle$, which is largest in magnitude when $\Delta q = u_i$. That is, if Δq is in the direction of u_i (away from q^*), then $J(u_i) = \lambda_i(t_f - t_0)/p$, since the columns of U are all orthonormal. Therefore, the maximal change in J is realized when Δq equals the column of U corresponding to the largest eigenvalue of $\mathbf{S}_q^T \mathbf{S}_q$.

A singular $\mathbf{S}^T \mathbf{S}$ would suggest that there are elements of q which locally act in a dependent manner, and we note that this dependent behavior includes the case where perturbations of at least one of the parameters in q locally incur no changes in the solution. Moreover, the presence of extraordinarily small eigenvalues in Λ would suggest a lack of importance of one or a combination of parameters, and indeed, we will encounter this case in the next section.

4.3. Results. Let us analyze the aforementioned delay differential equation model of HIV pathogenesis to illustrate the benefit of this analysis. Our goal in using the PCA is to ascertain which perturbed parameters and/or combinations of perturbed parameters have the most and least dramatic impact upon the solution near the best fit $q^* = (\delta^*, c^*, \tau^*) = (1.57, 4.3, 0.91)$ [data from patient 103 in Nelson *et al.* (2001)]. We begin by comparing the effects of δ and c and find that the eigenvectors of $\mathbf{S}_{[\delta,c]}^T \mathbf{S}_{[\delta,c]}$ are

$$U = \begin{bmatrix} -0.062 & -0.998 \\ -0.998 & 0.062 \end{bmatrix},$$

with corresponding eigenvalues $\lambda_1 \approx 3.6$, and $\lambda_2 \approx 165$. Clearly, the largest eigenvalue is λ_2 , which corresponds to u_2 , and implies that Δq will have the largest impact upon J if it is in the u_2 direction. If we change q^* in the direction of u_2 , this corresponds to perturbations of q^* such that the ratio between the first and the second components of Δq is maintained at $-0.062/0.998 \approx -0.0621$. Thus, to realize the maximal effect upon J , perturbed values of δ and c must follow the curve

$$c = -0.0621(\delta - \delta^*) + c^*, \quad (5)$$

while the minimal effect is realized by following

$$c = 16.1(\delta - \delta^*) + c^*. \quad (6)$$

The isocline contours of J , along with the major and minor axes of the approximating paraboloid of J are depicted in Fig. 4. These major and minor axes describe (locally) the directions of largest and smallest change in J and are parameterized by equations (5) and (6), respectively. To generate this contour plot, we simulated (1) with δ and c ranging over $[0.73, 2.57]$ and $[3.46, 5.06]$, respectively, and then used these simulations to compute the relative cost functional. In general, the computations necessary to generate the isoclines of J are inhibitory and would not

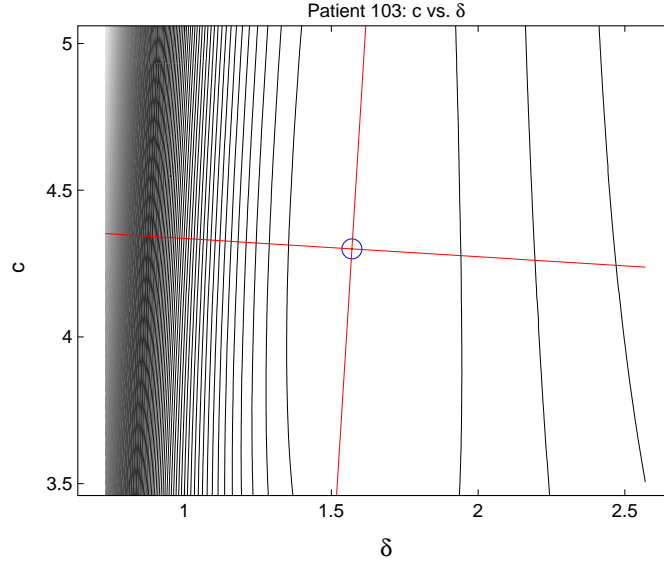


Figure 4. Contour plot of the isocontours of the relative cost functional J , where the circle represents the optimal point at $\delta = 1.57$ per day and $c = 4.3$ per day (with intercontour distance of 11.5 and maximum isocontour 1719.2). The (roughly) vertical and horizontal lines represent the major and minor axes of the approximating paraboloid and are described by equation (5), respectively.

readily be available; fortunately, our system is simple enough so as to make the calculations feasible. The depictions of these contours in this and all subsequent principle component analyses (Figs. 4–6) are provided merely to visually illustrate and verify our descriptions of the major and minor axes.

Next we compared the effects of δ and τ , and thus for $q = [\delta, \tau]$, we find that the eigenvectors of $\mathbf{S}_{[\delta, \tau]}^T \mathbf{S}_{[\delta, \tau]}$ are

$$U = \begin{bmatrix} -0.81 & -0.586 \\ -0.586 & 0.81 \end{bmatrix},$$

with eigenvalues of $\lambda_1 \approx 13.4$, and $\lambda_2 \approx 451$. Thus, to realize the largest effect upon J , perturbed values of δ and τ must follow the curve

$$\tau = -1.38(\delta - \delta^*) + \tau^*, \quad (7)$$

while the smallest effect is found on the curve

$$\tau = 0.723(\delta - \delta^*) + \tau^*. \quad (8)$$

The contours of J , along with the aforementioned curves are depicted in Fig. 5.

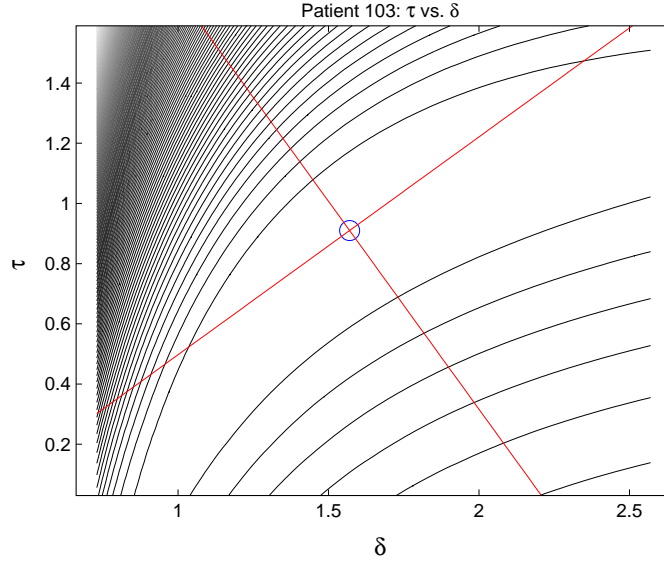


Figure 5. Isocline contour plot of the relative cost functional J , where the circle represents the optimal point at $\delta = 1.57$ per day and $\tau = 0.91$ days (with intercontour distance of 24.2 and maximum isocline 3632.45), along with major and minor axes of the approximating paraboloid.

If we compare c and τ , the resultant eigenvectors for $\mathbf{S}_{[c,\tau]}^T \mathbf{S}_{[c,\tau]}$ are

$$U = \begin{bmatrix} -0.99997 & 0.0075 \\ 0.0075 & 0.99997 \end{bmatrix},$$

with eigenvalues $\lambda_1 \approx 4.2$, and $\lambda_2 \approx 301$. Depicted in Fig. 6 are the contours of J , as well as the curves along which simultaneous changes c and τ result in maximal ($\tau = 133.2(c - c^*) + \tau^*$) and minimal ($\tau = -0.075(c - c^*) + \tau^*$) effects upon J .

Lastly, if we try to ascertain the three-way relationship between δ , c , and τ , we find an even more complex situation. In this case, we find that the eigenvectors of $\mathbf{S}_{[\delta,c,\tau]}^T \mathbf{S}_{[\delta,c,\tau]}$ are

$$U = \begin{bmatrix} 0.386 & -0.712 & -0.587 \\ 0.885 & 0.466 & 0.017 \\ 0.261 & -0.525 & 0.810 \end{bmatrix},$$

with eigenvalues $\lambda_1 \approx 0.5$, $\lambda_2 \approx 17$, and $\lambda_3 \approx 452$. The relationship here is not entirely clear, and thus while we can assert that the minimal effect upon J is observed by confining perturbations of the parameters to the plane described by

$$0.386(\delta - \delta^*) + 0.885(c - c^*) + 0.261(\tau - \tau^*) = 0,$$

this information does not readily lend itself to a biological interpretation.

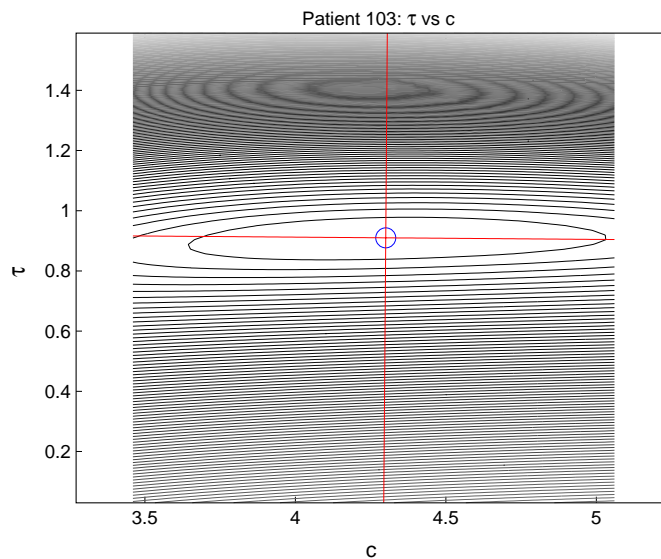


Figure 6. Isocline contour plot of the relative cost functional J , where the circle represents the optimal point at $c = 4.3$ per day and $\tau = 0.91$ days (with intercontour distance of 1.44 and maximum isocline 215.42), along with major and minor axes of the approximating paraboloid.

4.4. Discussion. Recall that the contour plots depict values of the *relative* cost functional and thus nonzero values of J represent a deviation of the differential equation dynamics away from a best fit to data solution. Therefore, if we consider the perturbations of parameters that result in a nominal change in J (and thus generate solutions close to the best fit), these ‘minimal effect’ curves [such as (8)], could in theory describe the presence or lack of biological relationships between infection parameters.

For example, consider the relationship between the infected T-cell death rate δ and the viral clearance rate c depicted in Fig. 4. The orientation of the major and minor axes of the paraboloid approximation to J suggest that δ and c are independent of one another. Indeed, from an immunological perspective, it can be shown that the dynamics of viral loads (for highly effective drug therapy) are controlled somewhat independently by δ and c [see Perelson and Nelson (1999)]. A similar situation is encountered when we consider the relationship between c and τ depicted in Fig. 6. The major and minor axes are nearly vertical and horizontal, respectively, thus suggesting that the impact of c and τ are also somewhat independent of one another. Thus, this sensitivity analysis suggests that the aspect of the dynamics controlled by c is intrinsically different from the aspects controlled by δ or τ , which coincides with our understanding that the value of c determines the rate of short-term decay [again, see Perelson and Nelson (1999)].

The relationship between δ and τ depicted in Fig. 5 is slightly different, since the parameters are clearly not independent. The delay τ describes the length of

the ‘shoulder’ depicted in Fig. 1(d), while the infected T-cell death rate δ determines the long-term dynamics of the viral population after the initiation of protease inhibitor therapy [as described in Nelson *et al.* (2000)]. According to our principle component analysis, in order to attempt to maintain a best fit, i.e., move in the direction of least change of J , an increase in δ must be matched by a corresponding increase in τ . This behavior is clearly depicted in Fig. 5, parameterized by the curve in (8), and supports the claim in Nelson and Perelson (2002), that for an imperfect drug ($n_p < 1$), the incorporation of a nonzero delay causes an increase in the best fit estimate of δ . As mentioned before, the contour plot of J is typically not calculated, however, we can do so for our problem because of the relative simplicity of our system. We note that the ‘basin’ of the contour plots represents the set of parameters corresponding to solutions of (1) close, in a least squares sense, to the best fit $x(t, q^*)$. The basins in Figs. 4 and 6 are roughly oval shaped, and the orientation of their major and minor axes along the vertical and horizontal directions, which correspond to our claim that c is locally independent of both δ and τ . The shape of the basin of ‘nearly best fit’ solutions in Fig. 5 is clearly not an oval and thus provides more support for the notion that δ and τ are dependent (and indeed suggests a nonlinear relationship).

Lastly, we note that among the sensitivity analyses found in the chemistry literature [such as Vajda *et al.* (1985), Vajda and Turányi (1986)], it is common to perform a change of variables on the parameters. In these papers, the authors let $q = e^\alpha$, define a new cost functional \tilde{J} such that $\tilde{J}(\alpha) = J(e^\alpha)$, and then expand a Taylor series around $\alpha^* = \ln(q^*)$. In this case, the expansion is

$$\tilde{J}(\alpha) = \tilde{J}(\alpha^*) + \nabla \tilde{J}(\alpha^*)(\alpha - \alpha^*) + \frac{1}{2}(\alpha - \alpha^*)^T \nabla^2 \tilde{J}(\alpha^*)(\alpha - \alpha^*) + \dots$$

They make the standard substitution for $\nabla^2 \tilde{J}$ [as in (4)], but we note that

$$\nabla^2 \tilde{J}(\alpha) \approx \text{diag}(q^*) R'(q^*)^T R'(q^*) \text{diag}(q^*),$$

where $R'(q^*)$ is defined as in Section 4.1 and $\text{diag}(q^*)$ is a diagonal matrix with q^* on the diagonal. In this situation, the eigenvectors define a ratio between powers of the parameters such as

$$\frac{\delta^* \ln\left(\frac{\delta}{\delta^*}\right)}{\tau^* \ln\left(\frac{\tau}{\tau^*}\right)} = -\frac{0.81}{0.586} \quad (9)$$

for the ratio between the powers on δ and τ . Similar to equations (7) and (8), the curves parameterized by

$$\tau = \tau^* \exp\left(-\frac{0.81\tau^*}{0.586\delta^*} \ln\left(\frac{\delta}{\delta^*}\right)\right) \quad (10)$$

and

$$\tau = \tau^* \exp\left(\frac{0.586\tau^*}{0.81\delta^*} \ln\left(\frac{\delta}{\delta^*}\right)\right) \quad (11)$$

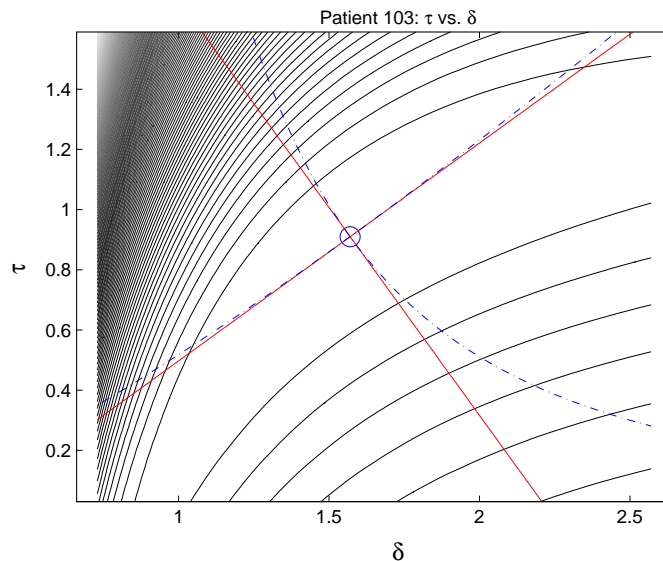


Figure 7. Isocline contour plot of the relative cost functional J , where the circle represents the optimal point at $\delta = 1.57$ per day and $\tau = 0.91$ days (intercontour distance of 24.2 and maximum isocline 3632.45). The solid lines are the linear relationships described by equations (7) and (8), and the nonlinear ‘dash-dot’ curves are the nonlinear relationships described by (10).

locally describe the ‘directions’ of largest and smallest change in \tilde{J} , respectively (see Fig. 7). It is tempting to believe that (10) is a nonintuitive (and clearly nonlinear) biological relationship. Unfortunately, the curves described by (10) and (11) do not actually offer any new insight into our problem, since the nonlinearity is merely a ramification of expanding a Taylor series in α as opposed to q . Moreover, the truncated Taylor series is only a reasonable approximation in a relatively small region of \mathcal{Q}_{ad} , and indeed for $\delta = 2$ and $\tau = 0.6$ the Lagrange remainder term for the Taylor series is already >87 . Thus this alternative approach is not useful in our situation.

5. CONCLUSIONS

While applying an analytical sensitivity analysis to a system of differential equations is clearly not a new idea, many of the available techniques have not been employed in studying models of disease pathogenesis. In this paper, we have applied differential analysis and principal component analysis to a recently published delay differential equation model of HIV infection dynamics. The results of our investigation support previous studies concerning the impact of δ and c and the importance of a nonzero τ as well as offers new insight into the nontrivial relationship between δ and τ .

The differential analysis presented in Section 3 suggests that near $c = 4.3$, $\delta = 1.57$, and $\tau = 0.91$, the infected T-cell death rate δ is most influential over the infected T-cell concentration T^* , while the viral clearance rate c is most influential over the infectious and noninfectious viral concentrations V_I and V_{NI} , respectively. The delay τ , however, strongly impacts on all compartments (after one day), thus supporting the claim from Nelson and Perelson (2002) that the inclusion of a nonzero delay is necessary due to its influence over the solution (and thus the fits to data).

The principal component analysis presented in Section 4 suggests that c is generally independent of δ and τ , whereas δ and τ maintain a relationship described (locally) by (8). The fact that δ and τ are correlated is not new, and indeed, with an imperfect drug, i.e., $n_p < 1$, it is known that the presence of a nontrivial delay in the dynamics indicates that a larger value of δ is needed to fit the data [again, see Nelson and Perelson (2002)].

While it is reassuring that the conclusions from this sensitivity analysis coincide with our current biological understanding of HIV infection dynamics, we hope that this application of sensitivity analysis also provides a good argument for these tools to see more widespread use in the disease modeling community.

ACKNOWLEDGEMENTS

P W Nelson is supported in part by a Career Award at the Scientific Interface from the Burroughs Wellcome Fund. D M Bortz is supported in part from a University of Michigan Rackham faculty development grant and also in part from the Burroughs Wellcome Fund.

REFERENCES

- Adelman, H. M. and R. T. Haftka (1986). Sensitivity analysis of discrete structural systems. *A.I.A.A. J.* **24**, 823–832.
- Banks, H. T. and D. M. Bortz. (2002). A parameter sensitivity methodology in the context of HIV delay equation models. *Technical Report CRSC-TR02-24*, Center for Research in Scientific Computation, North Carolina State University, Raleigh, NC (*J. Math. Biol.*, to appear).
- Bellman, R. and K. L. Cooke (1963). *Differential-Difference Equations*, Mathematics in Science and Engineering **6**, New York, NY: Academic Press Inc.
- Bortz, D. M. (2002). Modeling, analysis, and estimation of an *in vitro* HIV infection using functional differential equations, PhD dissertation, North Carolina State University, Raleigh, NC.
- Christie, S. H. (1833). The Bakerian lecture: experimental determination of the laws of magneto-electric induction in different masses of the same metal, and of its intensity in different metals. *Philos. Trans. R. Soc. Lond. Biol. Sci.* **123**, 95–142.

- Eslami, M. (1994). *Theory of Sensitivity in Dynamic Systems: An Introduction*, Berlin: Springer.
- Frank, P. M. (1978). *Introduction to System Sensitivity Theory*, New York, NY: Academic Press.
- Iman, R. L. and J. C. Helton (1988). An investigation of uncertainty and sensitivity analysis techniques for computer models. *Risk Anal.* **8**, 71–90.
- Kleiber, M., H. Antúnez, T. D. Hien and P. Kowalczyk (1997). *Parameter Sensitivity in Nonlinear Mechanics: Theory and Finite Element Computations*, New York, NY: John Wiley & Sons.
- Lazarides, A. A., H. Rabitz, J. Chang and N. J. Brown (1998). Identifying collective dynamical observables bearing on local features of potential surfaces. *J. Chem. Phys.* **109**, 2065–2070.
- Lazarides, A. A., H. Rabitz and F. R. W. McCourt (1994). A quantitative technique for revealing the usefulness of experimental data in refining a potential surface. *J. Chem. Phys.* **101**, 4735–4749.
- Lin, C. C. and L. A. Segel (1988). *Mathematics Applied to Deterministic Problems in the Natural Sciences*, Classics in Applied Mathematics **1**, Philadelphia, PA: Society for Industrial and Applied Mathematics.
- Moré, J. J. and S. J. Wright (1993). *Optimization Software Guide*, Frontiers in Applied Mathematics **14**, Philadelphia, PA: Society for Industrial and Applied Mathematics.
- Nelson, P. W., J. E. Mittler and A. S. Perelson (2001). Effect of drug efficacy and the eclipse phase of the viral life cycle on estimates of HIV viral dynamic parameters. *J. Acquir. Immune Defic. Syndr.* **26**, 405–412.
- Nelson, P. W., J. D. Murray and A. S. Perelson (2000). A model of HIV-1 pathogenesis that includes an intracellular delay. *Math. Biosci.* **163**, 201–215.
- Nelson, P. W. and A. S. Perelson (2002). Mathematical analysis of delay differential equation models of HIV-1 infection. *Math. Biosci.* **179**, 73–94.
- Perelson, A. S. and P. W. Nelson (1999). Mathematical analysis of HIV-1 dynamics *in vivo*. *SIAM Rev.* **41**, 3–44.
- Perelson, A. S., A. U. Neumann, M. Markowitz, J. M. Leonard and D. D. Ho (1996). HIV-1 dynamics *in vivo*: virion clearance rate, infected cell life-span, and viral generation time. *Science* **271**, 1582–1586.
- Saltelli, A., K. Chan and E. M. Scott (Eds), (2000). *Sensitivity Analysis*, Wiley Series in Probability and Statistics, New York, NY: John Wiley & Sons.
- Shampine, L. F. and S. Thompson (2001). Solving DDEs in Matlab. *Appl. Numer. Math.* **37**, 441–458.
- Stafford, M. A., L. Corey, Y. Cao, E. S. Daar, D. D. Ho and A. S. Perelson (2000). Modeling plasma virus concentration during primary HIV infection. *J. Theor. Biol.* **203**, 285–301.
- Stilianakis, N. I., K. Dietz and D. Schenzle (1997). Analysis of a model for the pathogenesis of AIDS. *Math. Biosci.* **145**, 27–46.
- Vajda, S. and T. Turányi (1986). Principal component analysis for reducing the Edelson-Field-Noyes model of the Belousov-Zhabotinsky reaction. *J. Phys. Chem.* **90**, 1664–1670.
- Vajda, S., P. Valko and T. Turányi (1985). Principal component analysis of kinetic models. *Int. J. Chem. Kinetics* **17**, 55–81.
- Wierzbicki, A. (1984). *Models and Sensitivity of Control Systems*, Studies in Automation and Control **5**, New York, NY: Elsevier Science Publishing Company Inc.

Zhou, W., R. A. Yetter, F. L. Dryer, H. Rabitz, R. C. Brown and C. E. Kolb (1998). Effect of fluorine on the combustion of 'Clean' surface boron particles. *Combustion Flame* **112**, 507–521.

Received 26 August 2003 and accepted 14 October 2003